Surface Science 299/300 (1994) 928–944
North-Holland

surface science

Metal–semiconductor contacts: electronic properties

Winfried Mönch
Laboratorium für Festkörperphysik, Universität Duisburg, D-47048 Duisburg, Germany

Received 18 March 1993; accepted for publication 20 August 1993

Rectification in metal–semiconductor contacts was first described by Braun in 1874. We owe the explanation of this observation to Schottky. He demonstrated that depletion layers exist on the semiconductor side of such interfaces. The current transport across such contacts is determined by their barrier heights, i.e., the respective energy difference between the Fermi level and the edge of the majority-carrier band. Since Schottky had published his pioneering work in 1938 the mechanisms, which determine the barrier heights of metal–semiconductor contacts, have remained under discussion. In 1947, Bardeen attributed the failure of the early Schottky–Mott rule to the neglect of electronic interface states. The foundations for a microscopic description of interface states in *ideal* Schottky contacts was laid by Heine in 1965. He demonstrated that a continuum of metal-induced gap states (MIGS), as they were called later, derives from the virtual gap states of the complex semiconductor band-structure. Neither this MIGS model nor any of the many other *monocausal* approaches, the most prominent is Spicer's Unified Defect Model, can explain the experimental data. In 1987, Mönch concluded that the continuum of MIG states represents the *primary* mechanism, which determines the barrier heights in ideal, i.e., intimate, abrupt, and homogeneous metal–semiconductor contacts. He attributed deviations from what is predicted by the MIGS model to other and then secondary mechanisms. In this respect, interface defects, structure-related interface dipoles, interface strain, interface compound formation, and interface intermixing, to name a few examples, were considered.

1. Introduction

The discovery of rectifying properties of metal–semiconductor contacts by Braun [1] in 1874 marks the beginning of semiconductor surface and interface physics. The technical importance of this *anomalous phenomenon* was soon realized. Large scale application of plate rectifiers based on cuprous oxide and later on selenium started as early as 1925 when a patent for such devices was issued to Grondahl [2].

A physical explanation of the *unilateral conduction* had to wait until Wilson [3] presented his quantum theory of semiconductors and the positive sign of the Hall coefficient and by this the p-type character of Cu_2O was finally established [4]. In his famous paper on the *Halbleitertheorie der Sperrschicht*, which was published by the end of 1938, Schottky [5] explained the blocking behavior of metal–semiconductor contacts by a space-charge layer on their semiconductor side which is depleted of mobile carriers. By now, this conclusion is easily derived.

In a Gedanken experiment, a metal–semiconductor contact may be created by gradually decreasing the distance between a metal and a semiconductor until eventually an intimate and abrupt interface has formed. This is illustrated in Fig. 1. The semiconductor is assumed to be non-degenerately doped n-type and to have no surface states within its band gap. The bands are thus flat up to the surface for infinite separation between metal and semiconductor.

The work functions of the metal and of the bare semiconductor generally differ so that in thermal equilibrium an electric field will exist in the vacuum gap between them. As a consequence, metal and semiconductor carry surface charges of equal density but of opposite sign. The condition of charge neutrality may be written as

$$Q_m + Q_{sc} = 0. \quad (1)$$

SSDI 0039-6028(93)E0514-U

In Fig. 1, the metal is assumed to have the larger work function. Then, the surface charge Q_m on the metal and Q_{sc} on the semiconductor have a negative and a positive sign, respectively.

The electric field enters both metal and semiconductor. However, the penetration depths are quite different. They scale with the Fermi–Dirac length of the metal and the Debye length of the semiconductor. Due to the large electron densities in metals, their screening lengths typically measure less than an ångström so that the field does not penetrate beyond the first atomic layer. For a doping level, for example, of 10^{17} cm^{-3} and room temperature, the Debye length amounts to typically 13.4 nm. Electric fields thus enter into non-degenerately doped semiconductors and, as a consequence, extended space-charge layers form. For the case assumed in Fig. 1, the space charge will be carried by positively charged donors. This is equivalent to a surface depletion of mobile electrons and an upward bending of the bands which increases the energy distance from the Fermi level to the conduction-band edge at the surface. This is the conclusion which was reached by Schottky in his famous paper mentioned above.

The current transport across such a depletion or Schottky barrier is governed by its barrier height or, as Schottky initially called it, its metal–semiconductor work function. The barrier height is defined as the energy distance between the Fermi level and the edge of the majority-carrier band, i.e.,

$$\phi_{Bn} \equiv W_{ci} - W_F \tag{2a}$$

and

$$\phi_{Bp} \equiv W_F - W_{vi}, \tag{2b}$$

where W_{ci} and W_{vi} denote the conduction-band minimum and the valence-band maximum at interfaces with n- and p-type doped semiconductors. For a specific metal–semiconductor pair, the experimental barrier heights ϕ_{Bn} and ϕ_{Bp} were always found to add up to the width of the bulk band gap of the semiconductor.

Since Schottky published his basic paper in 1938 the mechanisms determining the barrier heights in metal–semiconductor or Schottky contacts, as they are customarily named to honor Schottky's pioneering contribution to this field, have remained under discussion. In this contribution I will describe my view of the present understanding of this topic. For an extended review on metal–semiconductor contacts and a collection of most relevant papers in this field, the reader is referred to Refs. [6] and [7], respectively. More detailed presentations of specific aspects of semiconductor surface and interface physics may be found in Ref. [8].

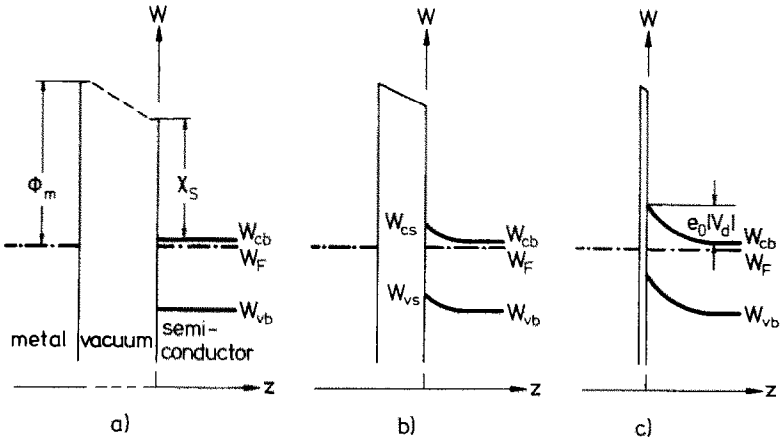

Fig. 1. Development of a Schottky barrier as a function of decreasing metal-to-semiconductor distance.

2. Determination of barrier properties

2.1. Barrier heights

Barrier heights in metal–semiconductor contacts may be evaluated from their
- current–voltage or I/V and
- capacitance–voltage or C/V characteristics as well as by
- internal photoemission and
- ballistic electron emission microscopy (BEEM).

The experimental data discussed in this paper were mostly derived from I/V and C/V characteristics. Therefore, these two methods shall be discussed briefly.

Current transport in Schottky contacts is due to majority carriers and, to a first approximation, it may be described by thermionic emission over the interface barrier. Tunneling through the barrier must be considered for high doping levels of the semiconductor, i.e., for narrow space-charge layers. For moderately doped n-type semiconductor substrates, the density of the thermionic emission current may be written as

$$j = j_0 \exp(e_0 V_a / n k_B T)[1 - \exp(-e_0 V_a / k_B T)], \tag{3}$$

with the saturation current density

$$j_0 = A_R^* T^2 \exp(-\phi_{Bn}^z / k_B T). \tag{4}$$

Here, A_R^* is the effective Richardson constant, n is the so called ideality factor, and ϕ_{Bn}^z is the barrier height at zero applied bias V_a. For a derivation of these relations the reader is referred to Refs. [9] and [10].

Recently, Sullivan et al. studied the current transport across homogeneous as well as inhomogeneous metal–semiconductor interfaces by numerical simulations [11]. Inhomogeneous Schottky contacts were modeled by patches with low barrier height which are embedded in a region with larger barrier height. Here, only the ideality factor and the *effective* barrier height are of interest. The ideality factor was obtained to be close to unity, typically $n < 1.03$, for homogeneous Schottky contacts, but becomes as large as 1.25 when the diameter of the patches measures 0.06 μm with all other parameters kept unchanged. Simultaneously, the *effective* barrier height of these patchy contacts decreased from the large value assumed for the embedding region to almost the smaller value chosen for the patches. The ideality factor and the effective barrier height were found to be almost linearly correlated. These results indicate that ideality factors n close to unity are a characteristic of homogeneous Schottky contacts. This result will be an important criterion for the selection of experimental barrier heights which will be considered in this paper.

The differential capacitance of the depletion layers in homogeneous Schottky contacts is obtained as

$$C_{dep} = [e_0^2 \epsilon_b \epsilon_0 N_d / 2(e_0 V_i - e_0 V_a)]^{1/2}, \tag{5}$$

where ϵ_b is the bulk dielectric constant. The extrapolated intercept on the abscissa of an $1/C^2$ versus V_a plot gives the interface band-bending,

$$e_0 V_i = \phi_{Bn} - (W_{cb} - W_F). \tag{6}$$

The energy distance $W_{cb} - W_F \equiv W_n$ from the Fermi level to the conduction-band minimum in the bulk is determined by the donor density N_d in the bulk. The flat-band barrier heights ϕ_{Bn} determined from the C/V characteristics of Schottky diodes are larger than their zero-voltage barrier heights ϕ_{Bn}^z evaluated from the respective I/V characteristics.

Ballistic electron emission spectroscopy (BEEM), a technique pioneered by Kaiser and Bell, utilizes the injection of electrons from a tip through a vacuum gap into the metal overlayer of Schottky contacts [12]. Provided the metal layer is sufficiently thin, a fraction of the injected electrons will reach the metal–semiconductor interface without scattering. These ballistic electrons will enter into the semiconductor only if their energy with respect to the Fermi level in the metal is larger than the barrier height of the contact or, in other words, if the voltage applied between the tip and the sample exceeds the barrier height. In patchy Schottky contacts, the length scale for the lateral resolution of BEEM is determined by the Debye length of the semiconductor and the extension of the depletion layer. However, irregularities of the metal film such as varia-

tions in thickness or chemical composition and grain boundaries will reduce the lateral resolution.

2.2. Chemical composition at metal–semiconductor interfaces

Physical models and explanations are always based on certain assumptions and idealizations. For the present case, intimate, abrupt, and homogeneous metal–semiconductor interfaces are the ideal. In general, both structural and compositional characterizations of metal–semiconductor interfaces are rather complicated and have been performed for specific cases only.

Chemical reactions were already detected in metal–selenium rectifiers by Poganski as early as 1952 [13]. Cd/Se rectifiers are the most prominent example. Just after metal evaporation their diode properties are poor but they are drastically improved by subsequent tempering at elevated temperatures. Careful studies revealed the formation of n-CdSe interlayers during such annealing treatments. In the resulting Cd/n-CdSe/p-Se sandwich structures, rectification occurs at the p-Se/n-CdSe heterojunction rather than at a metal–semiconductor interface.

During the past 40 years, quite a number of experimental techniques have been developed and improved for the determination of both the atomic arrangement and the chemical composition on surfaces which are either clean or covered with up to a few monolayers of adatoms. Typical and widely used structural probes are low-energy electron diffraction (LEED) and scanning tunneling microscopy (STM) while chemical surface compositions are routinely studied by electron-excited Auger electron spectroscopy (AES) and core-level photoemission spectroscopy (PES). These nondestructive techniques were also applied to follow the formation of metal–semiconductor interfaces. However, the applicability of electron-diffraction as well as electron-emission techniques in interface studies is principally limited by the escape depths of the electrons employed. For kinetic energies ranging between 50 and 2000 eV, the escape depths of electrons vary from 0.4 to 2 nm, respectively.

Alkali metals, which are evaporated on semiconductors and investigated at reduced temperatures, behave almost ideally in that they grow layer-by-layer. Already two layers, for example, of cesium atoms exhibit metallic behavior [14].

Most metals evaporated on semiconductor surfaces at room temperature form islands and, in some cases, it takes more than nominally 15 nm of metal deposited until the films eventually become continuous (see for example Ref. [15]). Chemical compositions at interfaces between continuous films of such metals and semiconductors can thus not be obtained by using the electron-emission spectroscopies mentioned above. Furthermore, data acquired at submonolayer coverages are not necessarily representative for real interfaces formed after evaporation of thicker metal overlayers. As an example, some results reported for GaAs and InP Schottky contacts shall be briefly mentioned. For a compilation of experimental data, the reader is referred to Ref. [16]. Many of the metals investigated were found to react with these compound semiconductors, i.e., chemical bonds at the semiconductor surface become disrupted. However, this does not necessarily imply that interfaces under thicker metal overlayers are intermixed. Most metals have larger surface free energies than gallium, indium, arsenic, and phosphorus [17,18]. Therefore, the latter atoms will segregate on surfaces of the growing metal islands and films. Furthermore, the solid solubility of the substrate atoms determines the extent to which they are dissolved in growing metal films.

Most of the 3d transition metal atoms evaporated on GaAs(110) surfaces at room temperature were found to replace surface Ga atoms [19]. Mostly, this cation exchange is limited to the top surface layer. The Ga atoms released first coalesce into islands and eventually segregate on top of the growing metal films.

Chemical compositions may also be evaluated utilizing destructive methods such as ion milling and secondary ion mass spectroscopy. The impinging ions not only remove surface atoms but also generate collision cascades in which the atoms are intermixed. These regions typically extend 2 to 5 nm below the surface. Thus, chemical

compositions at interfaces are difficult to evaluate from such data.

2.3. Atomic arrangements at interfaces

A typical experimental tool for the determination of surface structures is low-energy electron diffraction (LEED). Since the escape depths of the electrons used are small this technique is not suitable for interfaces between thick and continuous metal films and semiconductors. In recent years, X-ray techniques have been developed and considerably improved for the determination of surface and even interface structures. This progress is at least partly due to new and powerful X-ray sources such as electron storage rings. The potential of grazing-incidence X-ray diffraction was demonstrated by Hong et al. who investigated buried Ag/Si(111) interface structures [20]. The clean-surface Si(111)-7×7 reconstruction was found to persist under 26 nm of silver deposited at room temperature. Annealing of such films at 250°C, however, transformed the 7×7 into a 1×1 interface structure. The 7×7 structure has the lowest surface free energy of all clean-surface Si(111) structures but is obviously metastable under thick Ag films. The Si(111):Ag($\sqrt{3} \times \sqrt{3}$)R30° structure, which is obtained, for example, by deposition of a monolayer of Ag at 500 K, did not form. Quite on the contrary, the Ag-induced ($\sqrt{3} \times \sqrt{3}$)R30° structure is destroyed by further silver deposition even at room temperature. The conversion of the 7×7 to the 1×1 interface structure increases the barrier height by 0.05 eV from 0.69 to 0.74 eV [21].

The most interesting examples are the epitaxial $NiSi_2$/Si(111) interfaces. Such interfaces can be grown with a high degree of perfection. Cross-sectional investigations with high-resolution transmission electron microscopes revealed such interfaces to be abrupt and to grow in two different orientations of the epitaxial $NiSi_2$ films with respect to the underlying Si substrate. In type-A interfaces, the lattices are identically aligned on both sides of the interface while they are rotated by 180° around the interface normal for the case of type-B contacts [22,23]. Investigations of medium-energy ion scattering [24] as well as X-ray standing waves [25] confirmed that at both interfaces the Ni atoms are sevenfold coordinated. Rutherford backscattering provided upper limits of 1×10^{12} and 3×10^{13} Si atoms per cm^2 being displaced from lattice sites on the semiconductor side of type-A and type-B $NiSi_2$/Si(111) contacts, respectively [24]. Meanwhile it is well established that the barrier heights of the two types of $NiSi_2$/Si(111) contacts differ by 0.14 eV. Tung was the first to showthat they measure 0.65 eV for type-A and 0.79 eV for type-B interfaces prepared on samples doped n-type [26].

3. Mechanisms determining the barrier heights in Schottky contacts

3.1. No interface states: the Schottky–Mott rule

Schottky [5] proposed that rectification at metal–semiconductor contacts is due to the existence of depletion layers on the semiconductor side of such interfaces. Already a year later, Schweikert [27] reported a linear correlation between barrier heights measured with metal–selenium rectifiers and the work functions of the metals used. Such a chemical trend is obtained by quantifying the Gedanken experiment which is illustrated in Fig. 1 (see, for example, Ref. [6]).

In the vacuum gap between a metal and a semiconductor facing each other, an electric field exists due to the difference $\phi_m - \phi_{s0}$ of their work functions. The electric field penetrates into the semiconductor and its work function increases by the respective surface band-bending $e_0 V_d$. Since metals exhibit high densities of states at the Fermi level, the respective band bending at the metal surface will be extremely small and may be safely neglected. Therefore, the energy barrier across the vacuum gap, which amounts to $\phi_m - \phi_{s0}$ for infinite metal–semiconductor separation, reduces by $e_0 V_d$. Assuming the semiconductor and the metal to form a parallel-plate capacitor with plate separation d_{ms}, the surface charge densities on the semiconductor and the metal are given by

$$Q_{sc} = -Q_m = (\epsilon_0/e_0)[(\phi_m - \phi_{s0}) - e_0 V_d]/d_{ms}. \quad (7)$$

By solving Poisson's equation, the space-charge density in depletion layers is obtained as

$$Q_{sc} = +(2\epsilon_0\epsilon_b N_d e_0 V_d)^{1/2}, \quad (8)$$

for $e_0 V_d = W_{ci} - W_{cb} \geq 3k_B T$. By combining Eqs. (7) and (8), one obtains

$$[(\phi_m - \phi_{s0}) - e_0 V_d]^2 / e_0 V_d = 2e_0^2(\epsilon_b/\epsilon_0) N_d d_{ms}^2. \quad (9)$$

In the limit of an intimate contact, i.e., for $d_{ms} \to 0$, it follows

$$\phi_m - \phi_{s0} - e_0 V_d = 0. \quad (10)$$

The work function of a semiconductor, which has flat bands up to the surface, may be written as $\phi_{s0} = \chi_s + (W_{cb} - W_F)$, where χ_s is the surface electron affinity. Together with definition (2a) of the barrier height, Eq. (10) may be rewritten as

$$\phi_{Bn} = \phi_m - \chi_s, \quad (11)$$

which is the famous Schottky–Mott rule [28,29].

Barrier heights reported for GaAs Schottky diodes are displayed in Fig. 2. All data were evaluated from I/V curves. The ideality factors n ranged between 1.03 and 1.07. Thus, the data considered here originate either from homogeneous or from only slightly inhomogeneous Schottky diodes. To within 0.03 eV, which is the limit of experimental uncertainty, these flat-band barrier heights agree with respective values evaluated from C/V characteristics. Obviously, the experimental data are not described by the Schottky–Mott rule (11). As a trend, however, larger barrier heights seem to correlate with larger metal work-functions. There is no clustering of data points at or close to specific values. The experimental barrier heights rather scatter by 0.47 eV between 0.62 eV for Mg– and 1.09 eV for Ru–GaAs diodes. Schottky diodes were prepared on both {110}- and {100}-oriented substrates. Within the limits of experimental error, the data reveal no dependence of the barrier heights on the crystallographic orientation of the substrate surface. Details of the preparation, however, have a pronounced influence on the barrier height. In most cases, the metals were thermally evaporated. Electrochemical metal deposition, however, results in diodes with larger barrier heights compared with what is obtained when the metals are evaporated or even sputtered. Co/GaAs(001) Schottky diodes, for example, were prepared by thermal evaporation and electroless deposition of Co and were found to have barrier heights of 0.76 and 1.00 eV, respectively [30,31].

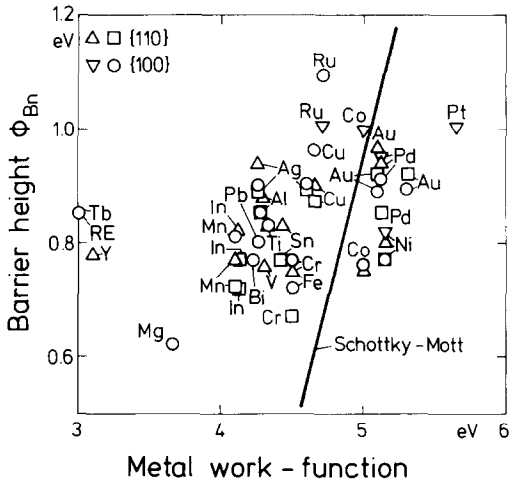

Fig. 2. Barrier heights of GaAs Schottky contacts as a function of the metal work-function. The straight line represents the Schottky–Mott rule. From Ref. [6].

3.2. The effect of a continuum of interface states on barrier heights

The barrier heights reported by Schweikert [27] for metal–selenium rectifiers certainly showed a linear correlation with the metal work-function but the slope $S_\phi = d\phi_{Bp}/d\phi_m$ was much smaller than unity as predicted by the Schottky–Mott rule (11). Later on, similar observations were made with other semiconductors. Bardeen [32] attributed the obvious discrepancy between the experimental barrier heights of metal–semiconductor contacts and the Schottky–Mott rule (11) to electronic interface states. Electronic interface states will absorb charge which has to be added to the condition of charge neutrality, i.e., Eq. (1) may be rewritten as

$$Q_m + Q_{is} + Q_{sc} = 0. \quad (12)$$

Since Q_m and Q_{is} reside on either side of the interface an electric double layer exists at

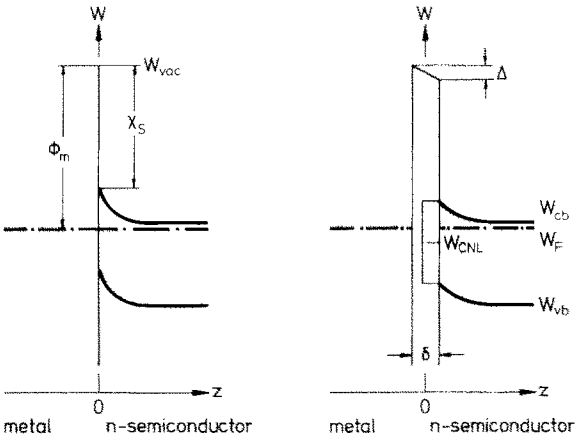

Fig. 3. Schematic band diagrams at intimate, rectifying metal–semiconductor contacts without and with electronic interface states.

metal–semiconductor interfaces. Its width δ_i is of atomic dimensions.

The effect of interface states on the barrier heights of metal–semiconductor contacts was first analyzed by Cowley and Sze [33]. They assumed a continuum of interface states with a constant density of states D_{is} across the band gap and a charge neutrality level W_{cnl}. For energies larger and smaller than W_{cnl}, the interface states have acceptor and donor character, respectively. The charge density in these interface states is then given by

$$Q_{is} = -e_0 D_{is}(W_F - W_{cnl}) = -e_0 D_{is}(\phi_{Bn}^0 - \phi_{Bn}), \tag{13}$$

where $\phi_{Bn}^0 \equiv W_{ci} - W_{cnl}$ is the barrier height for $Q_{is} = 0$, i.e., when no interface dipole exists and the Fermi level coincides with the charge neutrality level of the continuum of the interfaces states.

Fig. 3 displays band diagrams for rectifying metal–semiconductor contacts with and without interface states. The effect of interface states will be again analyzed for a parallel-plate-capacitor arrangement. The voltage drop across the interfacial double layer is related to the surface charge density as

$$\Delta = \phi_m - \chi_s - \phi_{Bn} = -(e_0/\epsilon_i\epsilon_0)Q_m\delta_i, \tag{14}$$

where ϵ_i is the dielectric constant of the interfacial layer. Inserting of Eqs. (8), (13), and (14) into the condition of charge neutrality (12) finally gives

$$\phi_{Bn} = S_\phi(\phi_m - \chi_s) - (1 - S_\phi)\phi_{Bn}^0, \tag{15}$$

with the slope parameter

$$S_\phi = \left[1 + (e_0^2/\epsilon_i\epsilon_0)D_{is}\delta_i\right]^{-1}. \tag{16}$$

The barrier heights are again linearly related to the work functions of the metals but the slope is reduced and depends on the density of states in the continuum of interface states. For $D_{is} = 0$, the slope parameter reaches its maximum value, $S_\phi = 1$, i.e., the Schottky–Mott rule is recovered. With $D_{is} \to \infty$, the barrier height becomes independent of the metal work-function, i.e., $S_\phi = 0$. Then, the Fermi level is pinned at the charge neutrality level of the interface states.

3.3. The continuum of metal-induced gap states

At clean metal surfaces or, in other words, at metal–vacuum interfaces, the wavefunctions of the electrons are exponentially decaying into vacuum. When the vacuum is replaced by a semiconductor or, more generally speaking, a dielectric the propagation of the wavefunctions across the solid–solid interface is somewhat more complicated. At the same time when Cowley and Sze analyzed the influence of a continuum of interface states on barrier heights in Schottky contacts, Heine [34] pointed out that at metal–semiconductor contacts a continuum of metal-induced interface states will exist. He argued that these states are derived from the virtual gap states (ViGS) of the complex band structure of the semiconductor.

Schrödinger's equation may be solved not only for real but also for complex wavevectors. For the bulk band structure, only real wavevectors are relevant since otherwise the Bloch functions cannot be normalized. Complex wavevectors mean that the wavefunctions decay or grow exponentially. Such behavior becomes meaningful at interfaces since the wavefunctions of real interface states will decay exponentially to both sides of the interface and are thus normalized. Such solutions of Schrödinger's equation with complex wavevec-

tors will have energy levels which lie within gaps of the bulk band structure. Therefore, these solutions of Schrödinger's equation are called virtual gap states (ViGS) of the complex band structure. Virtual gap states were first considered by Maue [35] for one-dimensional, linear chains of finite length by using the approximation of nearly free electrons. The respective ViGS wavefunctions may be written as

$$\psi(z) = A \exp(-qz) \cos(\pi z/a + \varphi), \qquad (17)$$

where A is a constant, φ is a phase factor which varies across the band gap, a is the lattice parameter of the chain, and q is the imaginary part of the wavevector.

With appropriate boundary conditions, real surface and interface states are derived from the continuum of virtual gap states. Real surface states at the ends of linear chains are obtained when one of the oscillatory solutions (17) can be fitted to a tail which exponentially decays into vacuum. Respective boundary conditions were derived by Maue [35]. With regard to interface states at metal–semiconductor interfaces, Heine [34] argued that

- in the energy range, where the metal conduction-band overlaps the semiconductor band-gap, the wavefunctions of the metal electrons decay into the semiconductor and
- these tails are to be described by the virtual gap states of the semiconductor band structure.

These metal-induced gap states (MIGS), as they were named later, form a continuum. They are occupied up to the Fermi level and empty above. Since the MIG states are derived from the bulk energy bands they will predominantly have donor character near to the valence-band maximum and acceptor character closer to the conduction-band minimum. The respective branch point is intuitively called the charge neutrality level of the ViGS. Charge neutrality levels of ViGS were computed first by Tejedor et al. [36] and later on by Tersoff [37] as well as Cardona and Christensen [38].

More realistic calculations of electronic properties of metal–semiconductor contacts were first performed by Louie and Cohen [40]. They considered Al–jellium/silicon contacts. Their calculations revealed four different types of electronic states to exist at such interfaces:

- In the energy region, where the conduction band of the metal overlaps the semiconductor valence-band, the states are matched and bulklike on either side of the interface.
- Below the bottom of the metal conduction-band, bulklike semiconductor states penetrate into the metal.
- Truly localized interface states, which decay to both sides of the interface, may be present in low-lying semiconductor band gaps.
- In the energy range where the metal conduction-band overlaps the energy gap of the semiconductor, the wavefunctions of the metal electrons tail into the semiconductor. This gives a continuum of metal induced-gap states (MIGS) which are occupied up to the Fermi level and empty above.

These calculations excellently confirmed Heine's conclusions which were based on simple physical concepts.

Recently, the existence of a continuum of metal-induced gap states was experimentally demonstrated by First et al. [41]. They evaporated submonolayer quantities of iron on cleaved GaAs(110) surfaces at room temperature and investigated the deposit with a scanning tunneling microscope. They found the evaporated iron atoms to coagulate in small epitaxial clusters. Islands with volumes larger than 1 nm^3 showed metallic behavior. Around such particles, metallic states detected on them were observed to overlap the semiconductor band gap in energy. These states decay exponentially as a function of distance away from the metallic iron islands. By using p- and n-type GaAs samples, occupied as well as empty gap states were probed. Experimental results published by First et al. are displayed in Fig. 4. The decay lengths of these gap states vary U-shaped across the GaAs energy gap with a minimum length of 0.34 nm near to mid-gap position. This experimental result is in excellent agreement with theoretical predictions. Already Maue [35] showed that the decay lengths $1/q$ of the ViGS vary U-shaped across the energy gap of one-dimensional chains. Louie et al. [42] studied Al–jellium/GaAs contacts by using a pseudo-

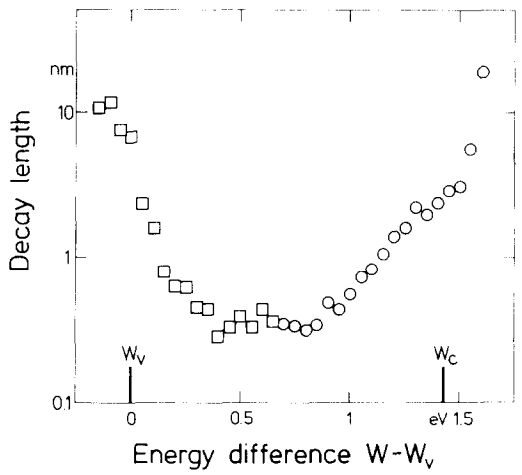

Fig. 4. Energy dependence of the decay length of gap states tailing away from metallic iron islands on cleaved GaAs(110) surfaces as determined by using a scanning tunneling microscope: (○) and (□) data recorded with samples doped p- and n-type. After First et al. [41].

potential approach. They obtained a U-shaped continuum of metal-induced gap states across the GaAs energy gap and a minimum decay length of 0.28 nm for the charge density in these MIGS. The continuum of gap states around metallic iron islands on cleaved GaAs(110) surfaces, which was directly observed by First et al. with a scanning tunneling microscope, exhibits all the features characteristic of the continuum of metal-induced gap states.

3.4. The electronegativity concept of charge transfer at metal–semiconductor interfaces

In their study on the influence of a continuum of electronic interface states on barrier heights in metal–semiconductor contacts, Cowley and Sze [33] made no assumptions on the physical nature of these states. Already Heine [34] identified them as the MIGS continuum. The charge in the MIGS or, in other words, the charge transfer across the interface determines the interface position of the Fermi level or, in other words, the barrier height. This is explained schematically in Fig. 5.

The Q_{gs}^{mi} versus W_F diagram on the right side of Fig. 5 immediately provides a chemical trend of barrier heights in Schottky contacts provided the charge transfer at metal–semiconductor interfaces is known. No such calculations have been

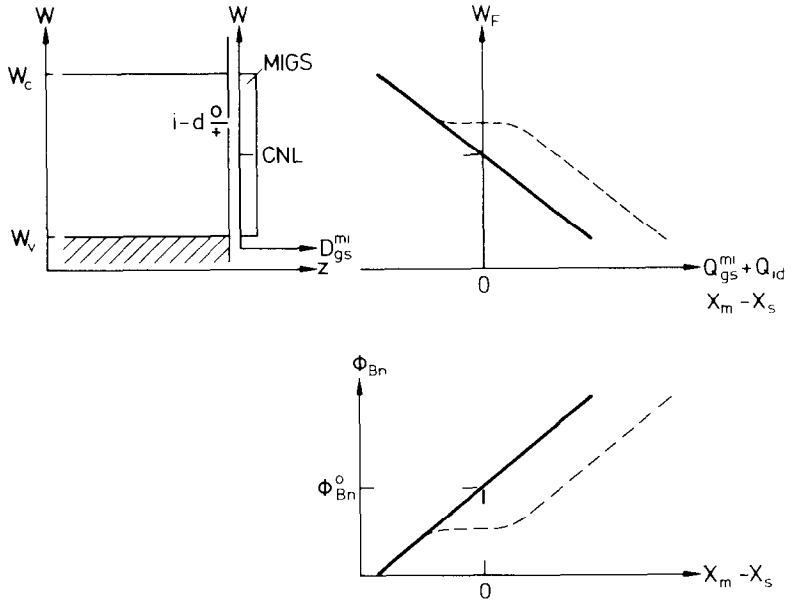

Fig. 5. Band diagram, charge transfer, and barrier height at metal–semiconductor contacts containing a continuum of interface states and interface defects of donor type in addition (schematically).

performed till now. Therefore, the present author extended Pauling's electronegativity concept of the partial ionic character of covalent bonds to semiconductor interfaces [39].

Pauling [43] correlated the ionicity Δq_1 of single bonds in diatomic molecules A–B between unlike atoms with the difference $X_A - X_B$ of the atomic electronegativities of the atoms forming the molecule. A revised version of the relation originally proposed by Pauling is that of Hanney and Smith [44]

$$\Delta q_1 = 0.16|X_A - X_B| + 0.035(X_A - X_B)^2. \quad (18)$$

In a simple point-charge model, the atoms are charged by $+\Delta q_1 e_0$ and $-\Delta q_1 e_0$, where the more electronegative atom becomes negatively charged. In a more realistic picture, the bond charge is slightly shifted towards the more electronegative atom in heteropolar diatomic molecules while it is in the middle between both atoms in homopolar diatomic molecules.

Pauling's concept proved to be useful also in solid state physics. Miedema and coworkers [45] applied it to metal alloys. The present author used it for modeling of the charge transfer across semiconductor interfaces [39] and proposed that to first approximation the charge transfer across metal–semiconductor interfaces varies proportional to the difference $X_m - X_s$ between the electronegativities of the metal and the semiconductor. For elemental semiconductors, their atomic electronegativities may be used. In generalizing Pauling's concept, the electronegativity of compounds is taken as the geometric mean of the atomic electronegativities of their constituents. For binary compounds one then obtains

$$X_{AB} = (X_A X_B)^{1/2}. \quad (19)$$

According to relation (18), the electronegativity concept of the charge transfer at metal–semiconductor interfaces assumes that the charge Q_{gs}^{mi} in the metal-induced gap states varies proportional to the electronegativity difference $X_m - X_s$. The W_F versus Q_{gs}^{mi} or, what is the same, W_F versus $(X_m - X_s)$ diagram on the right side of Fig. 5 now provides a chemical trend of the barrier heights of metal–semiconductor contacts. For $X_m - X_s = 0$, the Fermi level will coincide with the

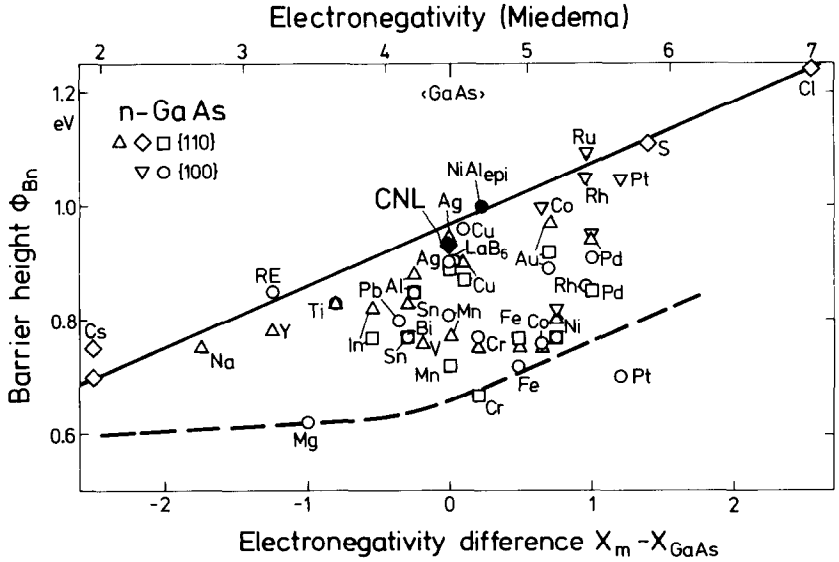

Fig. 6. Barrier heights reported for metal/GaAs contacts against the electronegativity difference $X_m - X_{GaAs}$ (Miedema electronegativities). From Refs. [6,44].

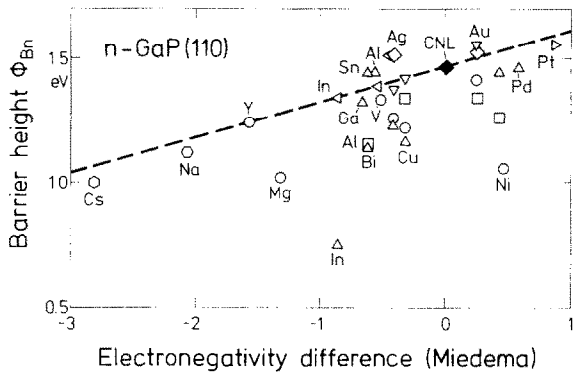

Fig. 7. Barrier heights reported for metal/GaP contacts against the electronegativity difference $X_m - X_{GaP}$ (Miedema electronegativities). From Ref. [14].

charge neutrality level of the MIG states. Thus, the barrier height will vary as

$$\phi_{Bn} = \phi^0_{Bn} + S_X(X_m - X_s), \qquad (20)$$

for semiconductors doped n-type. Eq. (20) is illustrated by the diagram in the lower right side of Fig. 5. Relation (20) explicitly states that the charge neutrality levels represent no *canonical pinning positions of the Fermi level* in metal–semiconductor contacts. According to Eq. (16), the slope S_X is determined by $D_{is}\delta_i/\epsilon_i$, i.e., by the product of the density of interface states and the width of the interface dipole layer divided by the interface dielectric constant.

There have been previous attempts to correlate barrier heights of Schottky contacts with metal electronegativities. These earlier ϕ_{Bn} versus X_m plots were still inspired by the Schottky–Mott rule in that they replaced the metal work-function by the metal electronegativity. By this, dipole contributions to the work functions, which are known to vary as a function of surface orientation, should remain disregarded. It shall be explicitly emphasized that the present correlation between barrier heights of Schottky contacts and the *difference* of the metal and semiconductor electronegativities *conceptually* differs from these

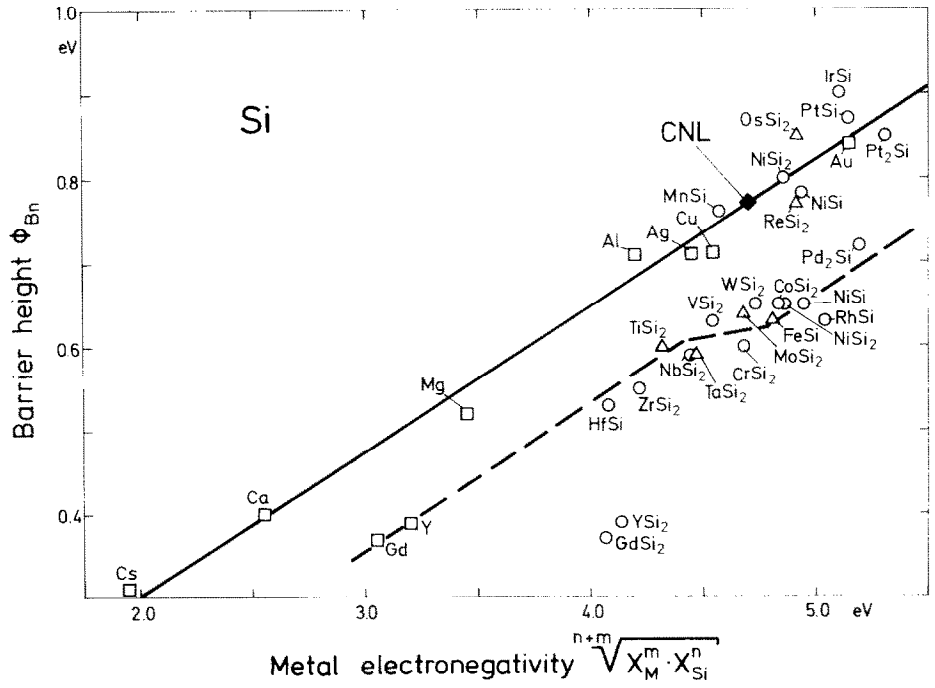

Fig. 8. Barrier heights reported for metal/Si and silicide/silicon contacts against the metal electronegativity $(X_m^m X_{Si}^n)^{1/(n+m)}$ (Miedema electronegativities). The charge-neutrality barrier height was entered at $X_{Si} = 4.7$. From Ref. [46].

earlier attempts. The present approach models the *charge transfer* between the metal and the metal-induced gap states of the semiconductor by the electronegativity difference $X_m - X_s$ and, therefore, it *predicts* the charge-neutrality barrier height ϕ_{Bn}^0 for metal–semiconductor pairs with $X_m - X_s = 0$.

In Figs. 6 to 8, barrier heights of GaAs [44], GaP [15], and Si [45] Schottky diodes are plotted as a function of the electronegativity difference $X_m - X_s$. The GaAs data are the same as in Fig. 2. All data were evaluated from I/V curves. Only the Cs/GaAs and Cs/GaP data were determined by using photoemission spectroscopy and a Kelvin probe. To obtain metallic cesium overlayers, the semiconductor substrates were held at low temperatures during Cs evaporation and subsequent measurements.

According to relation (20), the charge-neutrality barrier heights $\phi_{Bn}^0 = W_{ci} - W_{cnl}$ were entered at the electronegativity difference $X_m - X_s = 0$. Here, the charge neutrality levels of the ViGS evaluated by Tersoff [37] were used. The straight lines, which were drawn through the charge-neutrality points, represent upper limits of the barrier heights in GaAs, GaP as well as Si Schottky diodes. The arguments, which led to relation (20), suggest to assign these straight lines to the charging of the continuum of metal-induced gap states. Consequently, the present author proposed the continuum of metal-induced gap states to be the primary mechanism which determines the barrier heights in intimate, abrupt, and homogeneous Schottky contacts and deviations to lower barrier heights are attributed to other, secondary mechanisms which are effective in addition to the MIG states [46,47].

The conclusion just reached means that there is not just one physical mechanism which determines the barrier heights in metal–semiconductor contacts. In the past, always monocausal approaches were invoked to explain the nonuniform chemical trends observed with the barrier heights of Schottky contacts. Most theoreticians favored the continuum of metal-induced gap states, i.e., the MIGS model. A most prominent contender was Spicer's Unified Defect Model [48]. It postulates that the Fermi level becomes pinned at defect levels which are generated in the selvedge of the semiconductor during metal depositions. However, the experimental data obtained – and this is most important – with *Schottky diodes* do not support the Unified Defect Model. This does not mean that defects play no role in determining barrier heights in Schottky diodes.

The Effective Work Function Model of Freeouf and Woodall [49] was designed to preserve the Schottky–Mott rule. It proposes to replace the work function of the metal deposited by an effective work function. For this purpose, the formation of anion microclusters was assumed by either oxide contaminations or metal–semiconductor interactions at interfaces between gold and compound semiconductors. It was suggested to replace the metal work-function in Eq. (11) by the work function of the anions. Again, this model cannot account for the wealth of the experimental data. By the way, this model is almost equivalent to the common anion rule which is not supported by the experimental data either. This does not mean that anion aggregates play no role at all in determining barrier heights in Schottky contacts. However, there is no unambiguous experimental evidence for the existence of such microclusters at metal–semiconductor interfaces.

3.5. Mechanisms other than MIGS

The experimental data for GaAs, GaP, and Si Schottky contacts, which are displayed in Figs. 6 to 8, show deviations from the MIGS lines towards lower barrier heights. There are a number of mechanisms, which might reduce barrier heights in metal–semiconductor contacts, such as

- interface defects,
- structure-related interface dipoles,
- interface strain,
- interface compound formation, and
- interface intermixing,

to name a few examples. Some of these extrinsic mechanisms are also considered in discussions of the band line-up at semiconductor heterostructures. Here, only the influence of interface defects and of structure-related extra dipoles on the barrier height shall be discussed.

3.5.1. Interface defects

Interface defects at metal–semiconductor interfaces will become charged and have thus to be considered in the condition of charge neutrality at the interface. Relation (12) is then replaced by

$$Q_m + Q_{gs}^{mi} + Q_{id} + Q_{sc} = 0, \tag{21}$$

where Q_{id} is the charge density in interface defects. The charge density Q_m on the metal side is now balanced by $Q_s \equiv Q_{gs}^{mi} + Q_{id} + Q_{sc}$ on the semiconductor side of the interface.

The energy levels of adatoms on metal surfaces or, more generally speaking, of defects at metal–vacuum interfaces are customarily broadened into wide resonances due to the interaction of the atomic levels with the continuum of conduction-band states. The respective line widths amount to typically 1 eV. At metal–semiconductor interfaces, the interaction between the metal and defects in the semiconductor selvedge is screened by the interface dielectric function ϵ_i. Ludeke et al. [50] obtained $\epsilon_i \approx 4$. The interaction matrix element contains the Coulomb potential squared and, therefore, the broadening of defect levels at metal–semiconductor interfaces reduces to 60 meV [51]. Defects in Schottky contacts may thus be assumed to exhibit sharp levels.

The influence of donor-type defects on the barrier heights of metal–semiconductor contacts is illustrated in Fig. 5. Sharp donor levels are assumed above the charge-neutrality level of the continuum of metal-induced gap states. As long as that much negative charge is transferred to the semiconductor as to keep the Fermi level well above the defect level, all donors are neutral. With decreasing negative charge in the semiconductor, the Fermi level approaches the defect level and defects are gradually charged positively. As a result, the Fermi level becomes *intermediately pinned* at the position of the defect levels. When all defects are eventually charged the continuum of MIG states will again take up additional charge and will again determine the position of the Fermi level in the band gap as a function of charge on the semiconductor side of the interface. In the diagrams on the right side of Fig. 5, the dashed lines illustrate the influence of the donor-type defects on the Fermi-level position within the gap or, what is the same, on the barrier height as a function of the charge density $Q_{gs}^{mi} + Q_{id}$ on the semiconductor side of the interface. Evidently, interface donors are lowering the barrier heights with respect to what is found when no interface defects are present.

Discrete interface donors contribute a net charge per unit area

$$Q_{id} = +e_0 N_{id}\left[1 - f_0(W_{id} - W_F)\right], \tag{22}$$

where N_{id} and W_{id} are the area density and the energy levels of the interface defects, respectively, and $f_0(W_{id} - W_F)$ is the Fermi-Dirac distribution function. The maximum decrease $\delta\phi_{Bn}^{max}$ of the barrier height is achieved when all interface donors are charged, i.e., for $f_0 = 0$. By inserting Eqs. (8), (13), (14), and (22) into the condition of charge neutrality (21) one obtains

$$\delta\phi_{Bn}^{max} = -(1 - S_\phi) N_{id}/D_{gs}^{mi}. \tag{23}$$

The experimental data plotted in Figs. 6 to 8 give maximum barrier-height reductions of $\delta\phi_{Bn}^{max} \simeq -0.3$ eV. With $S_\phi = 0.2$ and $D_{gs}^{mi} = 3 \times 10^{14}$ cm^{-2} eV^{-1}, which are typical parameters, one obtains a density of approximately 1×10^{14} interface donors per cm^2. This simple estimate is in excellent agreement with results from more elaborate computations by Zhang et al. [52].

The reduced barrier heights in Figs. 6 to 8 with respect to the MIGS lines may thus be explained by defects of donor type. The estimated maximum density of 1×10^{14} cm^{-2} corresponds to approximately one tenth of a monolayer. As was pointed out earlier, such defects might be fabrication-induced. As possible candidates for such donor defects, Weber et al. proposed As_{Ga} antisite defects to exist in metal–GaAs contacts [53]. Since such defects are double donors, interface acceptors have to be present in addition [54]. Such As_{Ga} defects might also be described as anion microclusters. However, no fabrication-induced defects were identified at metal–semiconductor interfaces till now.

3.5.2. Structure-related interface dipoles

The barrier heights of type-B and type-A $NiSi_2$/Si(111) contacts measure 0.79 and 0.65 eV, i.e., they differ by 0.14 eV. These data were

first reported by Tung [26] and later on confirmed by many other groups. Fig. 8 reveals the data point for type-B interfaces to fit the silicon-MIGS line while type-A contacts deviate from it towards lower barrier heights. Furthermore, growth studies suggested that the interface free energy is lower for type-B than for type-A interfaces [55]. The reduced barrier height of type-A contacts cannot be attributed to interface defects. Medium-energy ion scattering studies performed by Fischer et al. gave an upper limit of 1×10^{12} displaced Si atoms per cm^2 [24]. By inserting such a low density of defects and the typical parameters used above into Eq. (23), one estimates a barrier-height decrease by 3 meV. Therefore, a mechanism other than defects has to be responsible for the reduction of the type-A barrier height in comparison with the one of type-B contacts which fits the silicon MIGS-line.

Besides defects, structure-related interface dipoles or, in other words, charge transfer across interfaces in addition to what results from the MIG states will also lead to variations in barrier heights. The present author proposed to describe such interface dipoles by an electric double layer [8]. The dipole moment $p_{i\perp}$ per interface atom may then be estimated by identifying dipole-induced variations of the barrier height by the potential drop across a dipole layer

$$\Delta\phi_{Bn}^{d} = \pm(e_0/\epsilon_i\epsilon_0)p_{i\perp}N_i, \tag{24}$$

where ϵ_i and N_i are the dielectric constant and the number of additional dipoles per unit area at the interface, respectively. The sign of the barrier-height variation depends on the orientation of the dipoles. Their moment may be approximated by

$$p_{i\perp} = e_0\Delta q_i d_i, \tag{25}$$

where $e_0\Delta q_i$ and d_i are the dipole charge and the dipole length, respectively. For the case of $NiSi_2$/Si(111) contacts, the dipole length is approximated by the Si bond length, the density of dipoles N_i is taken as the number of atoms per unit area in a Si(111) plane, and the interface dielectric constant is again assumed as $\epsilon_i \approx 4$ [50]. The barrier-height difference $\phi_{Bn}^{B} - \phi_{Bn}^{A} = 0.14$ eV then gives a charge

$$\Delta q_i^{A} \approx 0.017$$

for structure-related dipoles at type-A $NiSi_2$/Si(111) interfaces. The extra valence charge at interface atoms, which is attributed to structural differences between the two types of interfaces, is quite small. This estimate explains the great difficulties encountered in theoretical studies, which aim at computations of the barrier heights for type-A and type-B $NiSi_2$/Si(111) contacts, even if identical approaches such as the linear muffin-tin orbitals method in the atomic-sphere approximation or with a full-potential scheme are employed [56–58]. The barrier height of type-A interfaces turned out to be especially sensitive to variations of the interface geometry. This result is quite plausible since growth studies suggested that the interface free energy is lower for type-B than for type-A interfaces [55] and the extra charge transfer estimated above for this type of interfaces from the reduced barrier height is extremely small.

The electronegativity of $NiSi_2$ is larger than the one of silicon and, as a consequence, the charge in the MIG states is positive while a negative charge resides on the $NiSi_2$ side of the interface. Fujitani and Asano [56] confirmed this prediction by results from their computations mentioned above. The extra, structure-related dipoles are thus oriented such that they decrease the positive charge on the silicon side of type-A $NiSi_2$/Si(111) interfaces in comparison with type-B contacts.

3.6. *The slope parameter*

The MIGS model and the electronegativity concept of charge transfer at metal–semiconductor contacts describes the chemical trend of the respective barrier heights by the charge-neutrality barrier height $\phi_{Bn}^{0} = W_{ci} - W_{cnl}$ and the slope parameter $S_X = d\phi_{Bn}/dX_m$. This is illustrated by the diagram at the right bottom of Fig. 5. The charge neutrality levels W_{cnl} of the ViG states have been computed for many semiconductors [36–38]. This leaves the slope parameter to be discussed.

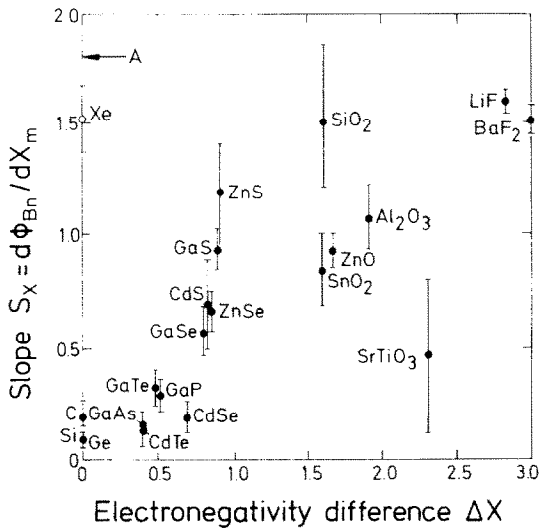

Fig. 9. Slope parameters $S_X = d\phi_{Bn}/dX_m$ as a function of the electronegativity differences of the constituent atoms of the semiconductors and insulators. After Kurtin et al. [59] and Schlüter [60].

In an early attempt, Kurtin et al. [59] evaluated slope parameters for some twenty different semiconductors and insulators and plotted them against the respective ionicities. Schlüter [60] reanalyzed these data and his revised set is displayed in Fig. 9. The data point for metal–xenon interfaces, which was obtained by Jacob et al. [61] some ten years later, clearly rules out the S-shaped trend which was inferred by Kurtin et al.

The present interpretation of the experimental data plotted in Figs. 6 to 8 concludes that barrier heights at abrupt metal–semiconductor interfaces are primarily determined by the charge transfer between the metal and the continuum of metal-induced gap states of the semiconductor. The ViG states of linear chains have a density of states which varies U-shaped across the band gap and is almost constant around the charge neutrality level over approximately half of the band gap. Therefore, it seems to be a reasonable assumption that the continua of metal-induced gap states also have almost constant densities of states near to their charge neutrality levels. This assumption is also justified by the experimental data of First et al. which are displayed in Fig. 4.

A model with a continuum of unspecified interface states at metal–semiconductor contacts was first considered by Cowley and Sze [33]. It is described in Section 3.2. This approach modeled the voltage drop across the interfacial dipole layer by the difference $\phi_m - \chi_s$. According to Eq. (16), the slope parameter $S_\phi = d\phi_{Bn}/d\phi_m$ is then determined by the product $D_{is}\delta_i$. Here, however, slope parameters $S_X = d\phi_{Bn}/dX_m$ are of interest. The slope parameters S_ϕ and S_X may be easily converted since the work functions and the electronegativities of metals are linearly correlated as was first pointed out by Gordy and Thomas [62]. A least-squares fit to the work functions of polycrystalline metals and the respective Pauling electronegativities gives

$$\phi_m = 1.79 X_{Paul} + 1.11 \text{ [eV]}. \quad (26)$$

Such a trend is easily explained. In a vacuum gap between two solids exhibiting different work functions, an electric field builds up. Due to this contact potential the material with the smaller and the larger work function will become charged positively and negatively, respectively. As in chemical bonds, this charge transfer again follows the sign of the electronegativity difference. By considering the empirical relation (26), Eq. (16) may be rewritten as

$$A/S_X - 1 = (e_0/\epsilon_i\epsilon_0) D_{is}(W_{cnl})\delta_i. \quad (27)$$

The coefficient A amounts to 1.79 when Pauling's and 0.93 when Miedema's electronegativities are used.

The present approach identifies the interface states with the continuum of MIGS. Then, the thickness δ_i of the interfacial dipole layer may be approximated by the decay length $1/q_{cnl}$ of the MIGS. For a one-dimensional linear chain, both $D_{gs}^{vi}(W_{cnl})$ and $1/q_{cnl}$ vary inversely proportional to the width of the respective energy gap. Therefore, it is expected that the slope parameters S_X will also be determined by the band gaps of the respective semiconductor substrates. In three-dimensional semiconductors, the width of the band gap varies across the Brillouin zone. Therefore, average band gaps have to be considered rather than the usual direct or indirect band gaps which are all referenced with respect to the valence-

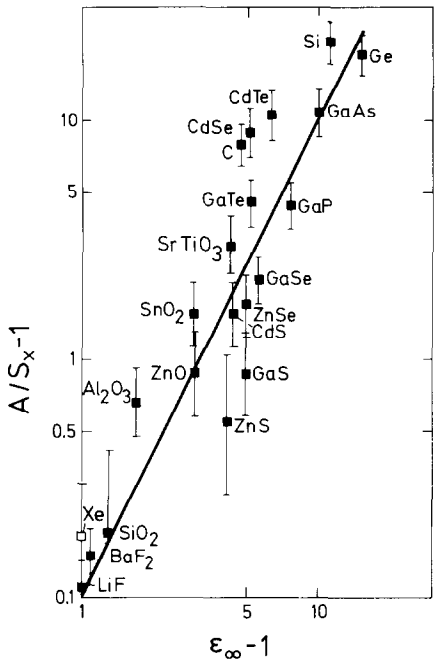

Fig. 10. Slope parameters $S_X = d\phi_{Bn}/dX_m$ (same data as in Fig. 9) as a function of the electronic susceptibilities $\epsilon_\infty - 1$ of the semiconductors and insulators. From Mönch [39].

band maximum in the middle of the Brillouin zone. The average band gap $\langle W_g \rangle$ is defined by

$$\epsilon_\infty - 1 = \left(\hbar\omega_p / \langle W_g \rangle\right)^2, \tag{28}$$

where ϵ_∞ is the electronic part of the static dielectric constant and $\hbar\omega_p$ is the energy of the plasmon of the bulk valence electrons. For the group IV and the III–V and II–VI semiconductors, the experimental plasmon energies vary by only $\pm 10\%$. Thus, the present author proposed that the slope parameter should obey a power law as a function of the susceptibility $\epsilon_\infty - 1$ [39], i.e.,

$$A/S_X - 1 \propto (\epsilon_\infty - 1)^n. \tag{29}$$

In Fig. 10, the same slope parameters, which are displayed in Fig. 9, are plotted over the electronic susceptibilities $\epsilon_\infty - 1$. Now, a distinct trend is obtained and a least-squares fit to the experimental data points yields

$$A/S_X - 1 = 0.1(\epsilon_\infty - 1)^{2.0}. \tag{30}$$

The regression coefficient is 0.91. The good correlation is not obvious since the S_X data exhibit large margins of experimental error and a large amount of scatter. Most importantly, the data point for metal–xenon interfaces now fits the trend. It shall be mentioned that the xenon data point was reported after the *semi-theoretical* relation (30) had been published. In agreement with relation (28), one finds $A/S_X - 1$ to vary proportional to $\langle W_g \rangle^4$. No such correlation is obtained when the same $A/S_X - 1$ data are plotted versus the widths of either the direct or the indirect band gaps. These findings strongly support the present approach that the charge transfer between the metal and the continuum of MIGS on the semiconductor side determines the barrier heights at metal–semiconductor interfaces and that the respective charge transfer may be modeled by the differences of the metal and semiconductor electronegativities.

References

[1] F. Braun, Pogg. Ann. 153 (1874) 556.
[2] L.D. Grondahl, U.S.Patent 160335 issued January 1, 1925.
[3] A.H. Wilson, Proc. Roy. Soc. (London) A 133 (1936) 458; 134 (1936) 277.
[4] O. Fritsch, Ann. Phys. 22 (1935) 375.
[5] W. Schottky, Naturwissenschaften 26 (1938) 843.
[6] W. Mönch, Rep. Prog. Phys. 53 (1990) 221.
[7] W. Mönch, Electronic Structure of Metal–Semiconductor Contacts (Kluwer, Dordrecht, 1990).
[8] W. Mönch, Semiconductor Surfaces and Interfaces (Springer, Berlin, 1993).
[9] S.M. Sze, Physics of Semiconductor Devices (Wiley, New York, 1981).
[10] E.H. Rhoderick and R.H. Williams, Metal–Semiconductor Contacts (Clarendon, Oxford, 1988).
[11] J.P. Sullivan, R.T. Tung, M.R. Pinto and W.R. Graham, J. Appl. Phys. 70 (1991) 7403.
[12] W.J. Kaiser and L.D. Bell, Phys. Rev. Lett. 60 (1985) 1406;
L.D. Bell and W.J. Kaiser, Phys. Rev. Lett. 61 (1988) 2368.
[13] S. Poganski, Z. Elektrochem. 56 (1952) 193; Z. Phys. 134 (1953) 469.
[14] R. Linz, H.J. Clemens and W. Mönch, J. Vac. Sci. Technol. B 11 (1993) 1591.
[15] D.E. Savage and M.G. Lagally, J. Vac. Sci. Technol. B 4 (1986) 943.
[16] Z. Lin, F. Xu and J.H. Weaver, Phys. Rev. B 36 (1987) 5777.
[17] A. Miedema, Z. Metallkd. 69 (1978) 287.
[18] L.Z. Mezey and J. Giber, Jpn. J. Appl. Phys. 21 (1982) 1569.

[19] F. Schäffler, G. Hughes, W. Drube, R. Ludeke and F.J. Himpsel, Phys. Rev. B 35 (1987) 6328.
[20] H. Hong, R.D. Aburano, D.-S. Lin, H. Chen, T.-C. Chiang, P. Zschack and E.D. Specht, Phys. Rev. Lett. 68 (1992) 507.
[21] R. Schmitsdorf, T.U. Kampen and W. Mönch, Proc. 1st Int. Conf. on Control of Semiconductor Interfaces, Karuizawa, Japan, November 8–12, 1993.
[22] D. Cherns, G.R. Anstis, J.L. Hutchinson and J.C.H. Spence, Phil. Mag. A 46 (1982) 849.
[23] J.M. Gibson, R.T. Tung and J.M. Poate, Mater. Res. Soc. Symp. Proc. 14 (1983) 395.
[24] J. Vriemoeth, J.F. van der Veen, D.R. Heslinga and T.M. Klapwijk, Phys. Rev. B 42 (1990) 9598.
[25] A.E.M.J. Fischer, E. Vlieg, J.F. van der Veen, M. Clausnitzer and G. Materlick, Phys. Rev. B 36 (1987) 4769.
[26] R.T. Tung, Phys. Rev. Lett. 52 (1984) 461.
[27] H. Schweikert, Verh. Phys. Ges. 3 (1939) 99. These results were published in Ref. [28].
[28] W. Schottky, Phys. Z. 41 (1940) 570.
[29] N.F. Mott, Proc. Cambridge Phil. Soc. 34 (1938) 568.
[30] J.R. Waldrop, J. Vac. Sci. Technol. B 2 (1984) 445.
[31] P. Allongue and E. Souteyrand, J. Vac. Sci. Technol. B 5 (1987) 1644.
[32] J. Bardeen, Phys. Rev. 71 (1947) 717.
[33] A.M Cowley and S.M. Sze, J. Appl. Phys. 36 (1965) 3212.
[34] V. Heine, Phys. Rev. 138 (1965) A1689.
[35] A.W. Maue, Z. Phys. 94 (1935) 717.
[36] C. Tejedor, F. Flores and E. Louis, J. Phys. C (Solid State Phys.) 10 (1977) 2163.
[37] J. Tersoff, Phys. Rev. Lett. 52 (1984) 465; Surf. Sci. 168 (1986) 275.
[38] M. Cardona and N.E. Christensen, Phys. Rev. B 35 (1987) 6182.
[39] W. Mönch, Festkörperprobleme (Advances in Solid State Physics) Vol. 26, Ed. P. Grosse (Vieweg, Braunschweig, 1986) p. 67.
[40] S.G. Louie and M.L. Cohen, Phys. Rev. B 13 (1976) 2461.
[41] P.N. First, J.A. Stroscio, R.A. Dragoset, D.T. Pierce and R.J. Celotta, Phys. Rev. Lett. 63 (1989) 1416.
[42] S.G. Louie, J.R. Chelikowsky and M.L. Cohen, Phys. Rev. B 15 (1977) 2154.
[43] L.N. Pauling, The Nature of the Chemical Bond (Cornell University, Ithaca, 1939/60).
[44] N.B. Hanney and C.P. Smith, J. Am. Chem. Soc. 68 (1946) 171.
[45] A.R. Miedema, F.R. de Boer and P.F. de Châtel, J. Phys. F (Metal Phys.) 3 (1973) 1558;
A.R. Miedema, P.F. de Châtel and F.R. de Boer, Physica B 100 (1980) 1.
[46] W. Mönch, Phys. Rev. B 37 (1988) 7129.
[47] W. Mönch, Phys. Rev. Lett. 58 (1987) 1260.
[48] W.E. Spicer, P.W. Chye, P.R. Skeath and I. Lindau, J. Vac. Sci. Technol. 16 (1979) 1422.
[49] J.L. Freeouf and J.M. Woodall, Appl. Phys. Lett. 39 (1981) 727.
[50] R. Ludeke, G. Jezequel and A. Taleb-Ibrahimi, J. Vac. Sci. Technol. B 6 (1988) 1277; Phys. Rev. Lett. 61 (1988) 601.
[51] R. Ludeke, in: Metallization and Metal–Semiconductor Interfaces, Ed. I.P. Batra (Plenum, New York, 1989) p. 39.
[52] S.B. Zhang, S.G. Louie and M.L. Cohen, Phys. Rev. B 32 (1985) 3955.
[53] E.R. Weber, H. Ennen, U. Kaufmann, J. Windscheif, J. Schneider and T. Wosinski, J. Appl. Phys. 53 (1982) 6140.
[54] W. Mönch, Surf. Sci. 132 (1982) 92.
[55] R.T. Tung, J.M. Gibson and J.M. Poate, Phys. Rev. Lett. 50 (1983) 429; Appl. Phys. Lett. 42 (1983) 888.
[56] H. Fujitani and S. Asano, Phys. Rev. B 42 (1990) 1696.
[57] G.P. Das, P. Blöchl, O.K. Anderson, N.E. Christensen and O. Gunnarsson, Phys. Rev. Lett. 63 (1989) 1168.
[58] S. Ossicini, O. Bisi and C.M. Bertoni, Phys. Rev. B 42 (1990) 5735.
[59] S. Kurtin, T.C. McGill and C.A. Mead, Phys. Rev. Lett. 22 (1970) 1433.
[60] M. Schlüter, Phys. Rev. B 17 (1978) 5044.
[61] W. Jacob, E. Bertel and V. Dose, Europhys. Lett. 4 (1987) 1303.
[62] W. Gordy and W.J.O. Thomas, Phys. Rev. 24 (1956) 439.